Linear Viscoelasticity and Time—Alcohol Superposition of Chitosan/Hyaluronic Acid Complex Coacervates

Linear Viscoelasticity and Time-Alcohol Superposition of Chitosan/Hyaluronic Acid Complex Coacervates

Juanfeng Sun, Jessica D. Schiffman, and Sarah L. Perry**

Department of Chemical Engineering, University of Massachusetts Amherst, Amherst, MA 01003, United States of America

*Corresponding authors: perrys@engin.umass.edu; schiffman@ecs.umass.edu

KEYWORDS: Complex Coacervation; Chitosan; Hyaluronic Acid; Linear Viscoelasticity; Rheology

ABSTRACT

Complex coacervation is an associative liquid-liquid phase separation phenomenon resulting from the complexation of oppositely-charged macro-ions. While it is well known that the phase behavior and rheological character of the resulting coacervates can vary as a function of the identity of the various species present (*i.e.*, macro-ions, salt, and solution conditions), the effect of solvent quality has been rarely studied. Here, the effect of adding small amounts of either methanol or ethanol to complex coacervates of the natural polymers chitosan and hyaluronic acid is described. The effect of cosolvent addition on the phase behavior and linear viscoelasticity of the resulting coacervates is characterized. Lastly, we explore the potential for using not only time-salt superposition,

but also time-alcohol and time-salt alcohol superposition to provide insight into coacervate rheology.

Sarah Perry 1/17/2022 8:11 PM
Deleted: new

Sarah Perry 1/17/2022 8:11 PM
Deleted: s

1. Introduction

Complex coacervation is an associative liquid-liquid phase separation phenomenon[1-3] driven by the complexation of oppositely-charged macro-ions that has found utility in fields ranging from adhesives,[4-7] to food and personal care products,[8-10] to medicine,[11-14] to materials.[15-23] The driving force for coacervation is a combination of electrostatic attraction and the subsequent entropic gains associated with the release of bound counterions and the restructuring of water upon complex formation.[1,24-27]

The importance of electrostatic and ionic effects has meant that the phase behavior and rheology of coacervates, particularly polymeric coacervates, has been studied as a function of the ratio of polycation to polyanion,[28-32] polymer length,[17,28,31,33-41] chemistry,[30,33,42-49] architecture,[50] pH,[28,32,51,52] salt concentration,[28,29,31,32,36,38,39,41,42,46,48,49,53-57] and salt identity.[29,40] However, very little experimental work to date has looked on the effect of different solvents, and therefore solvent quality and dielectric effects on the resulting coacervates.[25,58,59]

The electrostatic interaction between a single anion and cation can be described as by the Coulomb energy,

$$E = \frac{-e^2}{4\pi\varepsilon_0\varepsilon\sigma} = -\frac{l_B}{\sigma}kT \qquad (1)$$

where e is the elementary charge of the ions, σ is the separation distance between the ions, ε is the dielectric constant of the medium, and ε_0 is the dielectric permittivity of vacuum. This interaction can also be described in terms of the Bjerrum length (l_B).

$$l_B = \frac{-e^2}{4\pi\varepsilon_0\varepsilon kT} \quad (2)$$

At room temperature, the value of the dielectric constant for water is $\varepsilon = 80.1$, whereas for most organic solvents the value is much lower (*e.g.,* for ethanol $\varepsilon = 25.3$). Therefore, the addition of a miscible organic solvent would be expected to strengthen the electrostatic interactions between the various polyions and salts present in a solution, and thus, increase the stability of a complex coacervate (often described in terms of a salt resistance or the size of the two phase region, Figure 2a). This type of result has been reported for systems of relatively hydrophilic polymers, such as polypeptides[25] and polysaccharides,[18] though more extensive studies are needed.

While the Coulombic nature of complex coacervation has meant that nearly all reports of coacervates have been in water-based systems, a recent report by Lee *et al.*, demonstrated complex coacervation using a system of polymerized ionic liquids in two different organic solvents, hexafluoro-2-isopropanol (HFIP) and 2,2,2-trifluoroethanol (TFE).[60] The results of this study showed a clear relationship between the salt-stability of complex coacervates and the dielectric constant of the solvent. However, complex coacervation as a phase separation phenomenon involves both intermolecular interactions between the various charged species and questions related to the solubility of the various polymers in the solvent medium – an aspect of the phase behavior that is complicated in a mixed solvent system. To this end, Meng *et al.*, described how the addition of lower dielectric constant solvents affected the phase behavior of coacervates formed from relatively hydrophobic, styrenic polyelectrolytes.[59] Coacervates prepared in a "less hydrophobic" ethylene glycol mixture had a higher salt resistance than those formed in an equivalent ethanol/water mixture. This result counters what would be expected if purely

electrostatic interactions were to dominate. However, the decreased polarity of the ethanol/water mixture could serve as a better solvent for more hydrophobic polymers, helping to facilitate the transition from a phase separated coacervate to a single-phase solution.

The potential for solvent effects was further highlighted in work by Danielsen *et al.*, who studied the complexation of poly(styrene sulfonate) with a conjugated polycation.[58] This work explored the phase behavior of the resulting polyelectrolyte complexes in the context of a tetrahydrofuran (THF)/water cosolvent system. Interestingly, liquid complex coacervates occurred at high concentrations of THF, whereas solid precipitates were observed for samples prepared at a higher water content, and thus, higher dielectric constant. Furthermore, the authors quantified the partitioning of water and THF between the polymer-rich complex phase and the polymer-poor supernatant, with the higher levels of THF in the coacervate phase presumably helping to solubilize the relatively hydrophobic polymers. Were this solvent partitioning reversed, one would have expected to observe a decreased tendency towards phase separation because of preferential polymer solubility in the single phase solution (Figure 2a).

The interplay between coacervate phase behavior and rheology has also been an area of active research.[18,33,35,38-41,44,51,54,55,57,61-64] While significant efforts have been reported with regards to polymer and salt effects, to date, minimal work has been reported on the effect of solvent and/or dielectric effects. However, the dielectric effects that have been shown to affect phase behavior would also be expected to affect the rheological response of the coacervates by altering the friction of the "sticky" electrostatic interactions between chains.[35,39,41,64]

Previously, we provided the first demonstration that nanofibers could be electrospun from complex coacervates formed from the medically-relevant biopolymers, chitosan and hyaluronic acid.[18] Notably, optimizing the rheology necessary to fabricate nanofibers from one solution that contains two oppositely charged polymers is not yet understood. In determining the solution properties required for electrospinning, we noted that salt and alcohol concentration affected the phase behavior and linear viscoelasticity of the biopolymers (Figure 1). Here, we systematically study how salt and alcohol affect the rheology of these complex coacervates. In particular, we explore the potential for combining time-salt superposition with time-alcohol superposition to enable a broader description of complex multi-component systems that could potentially help researchers to better understand the processing of coacervate materials across a range of applications.

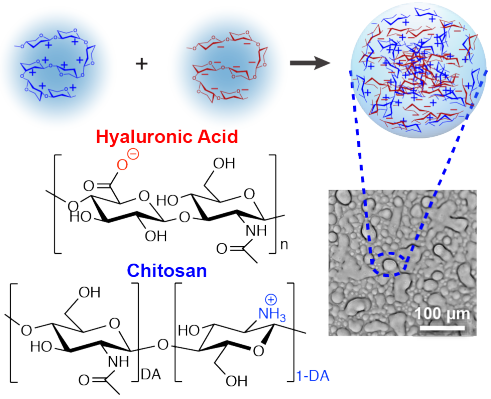

Figure 1. Schematic depiction of complex coacervation resulting from the interaction of the oppositely-charged polyelectrolytes in an aqueous solution alongside the molecular structures of chitosan and hyaluronic acid. The degree of acetylation (DA) of chitosan is the fractional number of acetylglucosamine units in the polymer. The optical micrograph shows liquid complex coacervates formed from 10 mM chitosan and hyaluronic acid and 500 mM NaCl, pH 4.5.

2. Experimental

2.1. Materials

Chitosan with a degree of deacetylation in the range of 75-85% and an average molecular weight of 50-190 kDa (Sigma-Aldrich) was dissolved in a pH = 4.5 solution. After dissolution, the solution was filtered through a 0.45 μm pore size filter (Millipore Express). Sodium hyaluronate with an average molecular weight of 199 kDa (Lifecore Biomedical) was dissolved in a solution that had a pH = 4.5, and was filtered through a 0.22 μm pore size filter (Millipore Express) prior to use. Sodium chloride (NaCl, ACS-grade), hydrochloric acid (HCl), sodium hydroxide (NaOH), methanol, and ethanol were used as received from Fisher Scientific. Deionized (DI) water was obtained from a Barnstead Nanopure Infinity water purification system (ThermoFisher Scientific).

2.2. Chitosan/Hyaluronic Acid Complex Coacervate Preparation and Characterization

Stock solutions of chitosan and hyaluronic acid were prepared gravimetrically at 60 mM on an ionizable monomer basis (*i.e.*, the concentration of chitosan was adjusted to take into account the fraction of deacetylated groups). An aqueous solution of 5 M NaCl was prepared gravimetrically, and all solutions were adjusted to pH 4.5 by adding concentrated HCl or NaOH. Complex coacervates were prepared by first combining the NaCl solution with water in a Falcon round bottom tube (14 mL, Fisher Scientific), followed by methanol or ethanol. Chitosan and hyaluronic acid were then added sequentially (in a 1:1 charge ratio unless otherwise specified) at a total ionizable monomer concentration of 40 mM. The mixture was vortexed for 10 s immediately after the addition of each solution to ensure complete mixing. After coacervate formation,

samples were then centrifuged (Sorvall Legend X1r Centrifuge, ThermoFisher Scientific) at 2000 rpm (750 × g) for 15 min to separate the dense coacervate phase**.**

Samples for turbidity and optical microscopy were prepared using the same method described above, but at a smaller scale (120 μL) and a total polymer concentration of 1 mM monomer. Immediately after their preparation, three 35 μL aliquots of each sample were pipetted into a 384-well plate (Falcon). Turbidity measurements were performed using a microplate reader (BioTek Synergy H1) at a wavelength of 562 nm. Samples were then inspected visually using optical microscopy (EVOS XL Core) to confirm the presence or absence of phase separation, as well as the liquid or solid nature of complexes that might have formed.

The linear viscoelasticity of the complex coacervates was determined using small-amplitude oscillatory shear measurements on a Malvern Kinexus Pro stress-controlled instrument. Strain amplitude measurements were first conducted to determine the appropriate strain rate to use within the linear viscoelastic region. Next, frequency sweeps were conducted over the range of frequencies from 100 to 1 (rad s^{-1}). Chitosan/hyaluronic acid coacervates prepared at 300 mM to 600 mM NaCl were studied using a 20 mm diameter stainless steel parallel plate fixture with a solvent trap whereas a 50 mm 2° core-and-plate fixture was used for samples prepared at 700 mM NaCl. Duplicate experiments were conducted. Data analysis was supported by the IRIS Rheo-Hub software (Interactive Rheology Information Systems Development LLC).

3. Results and Discussion

Here, we systematically explore how salt and various alcohols affect the linear viscoelastic response of complex coacervates formed from hyaluronic acid and chitosan (Figure 1). In our previous work, we used coacervation to facilitate the electrospinning of chitosan and

hyaluronic acid to create non-woven fibers that harness the demonstrated potential of these natural biopolymers in wound healing applications.[18,65,66] While conducting electrospinning experiments, we noted that cosolvents seemed to influence the rheology of the precursor solution and consequently the processing of coacervates into fibers; however, fully exploring that phenomena was beyond the scope of the electrospinning work.[18] It is worth noting that the complexity of biopolymers tends to complicate fundamental studies because of factors, such as polydispersity and the less well-defined chemical nature of biopolymers. For instance, chitosan is a copolymer of 2-acetamide-2-deoxy-β-D-glucopyranose and 2-amino-2-deoxy-β-D-glucopyranose (Figure 1) and has a blocky distribution of monomers along the chain that complicates questions of homogeneity. Furthermore, while most studies of coacervates tend to focus on Coulombic effects, there is a significant potential for hydrogen bonding in the chitosan/hyaluronic acid system. Thus, while our ultimate goal would be to identify potentially universal strategies, such as time-salt and time-alcohol superposition that can be applied to all coacervate systems, this first study highlights exciting avenues for future work.

Previous work by Kayitmazer *et al*., reported a pKa for chitosan of 6.4 with a degree of deacetylation of 83%, and a range of pKa values for hyaluronic acid from 2.4−2.9, depending on the polymer molecular weight.[67] Based on these results, we elected to operate at a solution pH of 4.5, which was both halfway in between, and approximately two pH units away from the pKa values for the two polymers. At these conditions, we used the simplifying assumption that all of the possible ionizable groups on the two polymers were charged, and samples were prepared at a 1:1 charge ratio of the two polymers.

The phase behavior of complex coacervates is generally described in terms of polymer and salt concentrations at fixed solution conditions and a specified ratio of polycation to polyanion. As shown schematically in Figure 2a, the two-phase region is located underneath a binodal curve. Samples prepared within this two-phase region will phase separate into a polymer-rich coacervate phase and a polymer-poor supernatant. Less intuitively, samples prepared at the same overall polymer concentration, but at increasing concentrations of salt are generally expected to form coacervates with decreasing concentrations of polymer through a process known as "self-suppression."

Rather than mapping out the entire two-phase region, experiments at low polymer concentrations that identify the location of the binodal curve are often used to identify trends in the phase behavior that are expected to generally track with those for the larger phase envelope.[17,25,33,37,68] We used simple, easy to conduct turbidity measurements, coupled with optical microscopy to identify the concentration of salt above which phase separation was no longer observed (*i.e.*, the salt resistance) for different concentrations of added methanol and ethanol. These data correspond to points on the polymer-poor branch of the binodal curve, and show a trend of increasing salt resistance with increasing alcohol concentration (Figure 2b).

Interestingly, the salt resistance values for ethanol were lower than those for methanol at the same concentration. This result would not be anticipated based on a purely dielectric argument (Figure 2a). In fact, a plot of salt resistance as a function of dielectric constant, calculated as a weighted average of the pure solvent values (Tables S1, S2) shows a significant divergence in the data for methanol as compared to ethanol (Figure 2c). Thus, while the trends in salt resistance appear to have some correlation with

dielectric constant, it appears that simple consideration of only the average solvent dielectric constant is insufficient to describe the resulting effect on coacervate phase behavior.

One potential explanation for this discrepancy could be the tendency of the various cosolvents to partition differently into the coacervate phase. This kind of selective cosolvent partitioning has been reported previously by Danielsen *et al.*[58] While such quantification is beyond the scope of the current work, we hypothesize that the higher salt resistances observed in the presence of methanol as compared to ethanol (Figure 2b) could be a consequence of stronger partitioning of methanol into the coacervate phase. A second possibility relates to the ways in which cosolvent addition affects the local structuring of water around the polymer and salt, and how such changes could affect the driving force for complexation.[27] Overall, it is likely that both factors have some effect on the observed phase behavior, and a detailed study into this question would provide valuable insight to the field.

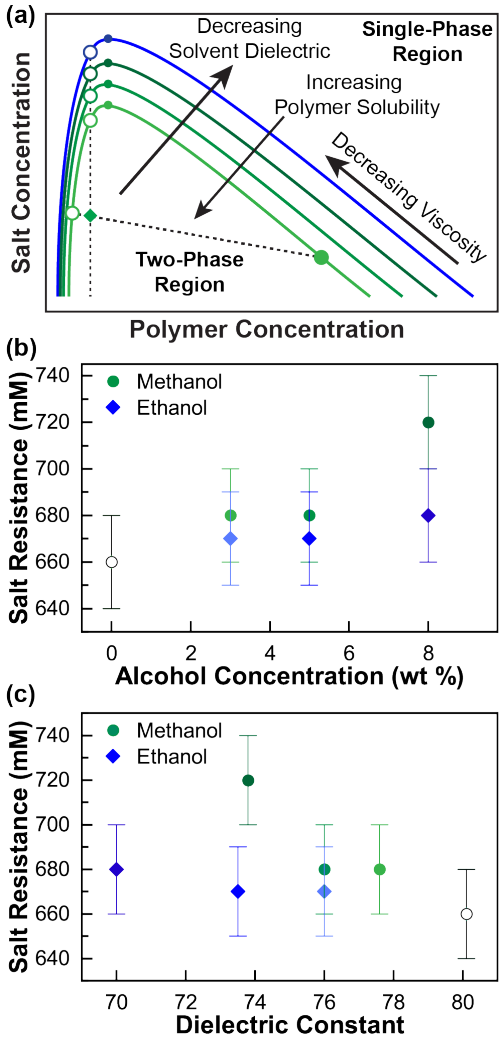

Figure 2. (a) Schematic depiction of the thermodynamic phase diagram for complex coacervation as a function of salt and polymer concentration (at a given temperature, polymer composition, pH, etc.). A sample prepared at a concentration within the two-phase region beneath the phase boundary will separate along tie-lines into a polymer-rich complex coacervate phase (closed circle) and a polymer-poor supernatant (open circles). To a first approximation, the size of the two-phase region would be expected to increase with decreasing dielectric constant of the solvent, or decrease with increasing polymer solubility, and can be described by a salt resistance determined at a constant polymer concentration. The viscosity of the coacervate is also expected to decrease with increasing salt concentration, due to the commensurate decrease in polymer concentration and electrostatic effects. Plots of **(b)** salt resistance vs. alcohol

concentration and **(c)** salt resistance vs. dielectric constant for coacervates prepared at 1 mM total ionizable monomers. Error bars correspond to error associated with the spacing between samples.

We then characterized the linear viscoelasticity of coacervates formed at varying salt concentrations and in the presence of increasing amounts of methanol and ethanol. The overall shape of the curves was typical of a polymer melt or solution, with the viscoelastic response being dominated by the loss modulus (G") at low frequency and the storage modulus (G') at high frequency. As expected, we observed a decrease in the storage and loss moduli with increasing salt concentration (Figures 3a-c and S1a, S2a-c, S3a-c). We also observed a shift in the frequency at which the crossover between moduli was observed, providing further evidence for faster relaxing, more liquid-like coacervates at higher salt concentrations. Similar trends were observed as a function of increasing salt concentration, regardless of the amount and/or identity of the cosolvent present.

We performed a time-salt superposition as a strategy for describing the response of our coacervate materials over a wider range of frequencies than was accessible for a single sample (Figures 3d-f and S1b, S2d-f, S3d-f).[33,35,39,41,55,61] This superposition requires both a horizontal and a vertical shift to account for salt-induced changes in the relaxation behavior of the material, and the concentration of polymer. The horizontal shift factor (*a*) showed the expected trend of decreasing magnitude with increasing salt concentration, while the vertical shift factor (*b*) increased with increasing salt concentration (Figures 3g-i, S1c, S2g-i, S3g-i). Using 600 mM NaCl as a common reference point, we also observed a trend of decreasing horizontal shift factor and increasing vertical shift factor with increasing concentration of alcohol (Figure S4).

In general, for any superposition, there is a requirement that the sample remain self-similar at all conditions (*i.e.*, that the morphology of the polymers remains

unaffected, or that the relaxation modes in the material have the same dependence).[69] This determination is typically conducted via either examination of the smoothness of the resulting superposed tan(δ) curves (Figures 3d-f, S1b, S2d-f, S3d-f), or via a graph of G" vs. G', a Cole-Cole plot (Figure S7). While time-salt superposition has been applied successfully across a range of coacervates formed from various synthetic polymers, we observed some deviations in the tan(δ) curves of our time-salt superposition data on the lower frequency end of the datasets, regardless of alcohol content. Analysis of the data using a Cole-Cole plot showed a smooth superposition for all of our samples (Figure S7), strongly supporting the idea that our approach is valid and that the deviations in tan(δ) at low frequencies may be a result of limitations in our experimental setup. Had deviations been observed in the Cole-Cole plot, this could have been evidence for microheterogeneities in the sample that could affect the validity of the superposition. While further study, particularly taking advantage of strategies such as time-temperature superposition to facilitate data collection over a wider range of frequencies,[56,62,64] would be needed to elucidate the reasons for the deviations in tan(δ), we have elected to proceed with the analysis, having acknowledged the potential limitations of our experimental setup and the frequency ranges that we can reliably acquire using our current rheometer.

In terms of the potential time-salt superposition of our data, it is worth noting that previous reports have described a range of different scaling behaviors for the horizontal shift factor as a function of salt concentration.[35,39,41,54,55,57] The theory used to originally develop time-salt superposition predicts a dependence of the form $a \sim \exp\left(-\sqrt{C_s}\right)$.[35,41] As presented, our data appear to indicate an exponential dependence on the salt concentration C_s (*i.e.*, linear on a semi-log plot). However, we note that our data are graphed as a function of the as-prepared concentration of salt, and that we did not directly measure the

amount of salt in the coacervates or take into account the counterions introduced by the polymers themselves. Such considerations could alter the observed scaling behavior, but previous work suggested that the overall shape of the trend is likely similar.[55] It is also interesting to note that the magnitude of the slope of both the horizontal and vertical shift factors generally decreases with increasing alcohol content (Figures S2g-i and S3g-i), perhaps suggesting that the decreased dielectric environment is less sensitive to salt-induced acceleration and swelling.

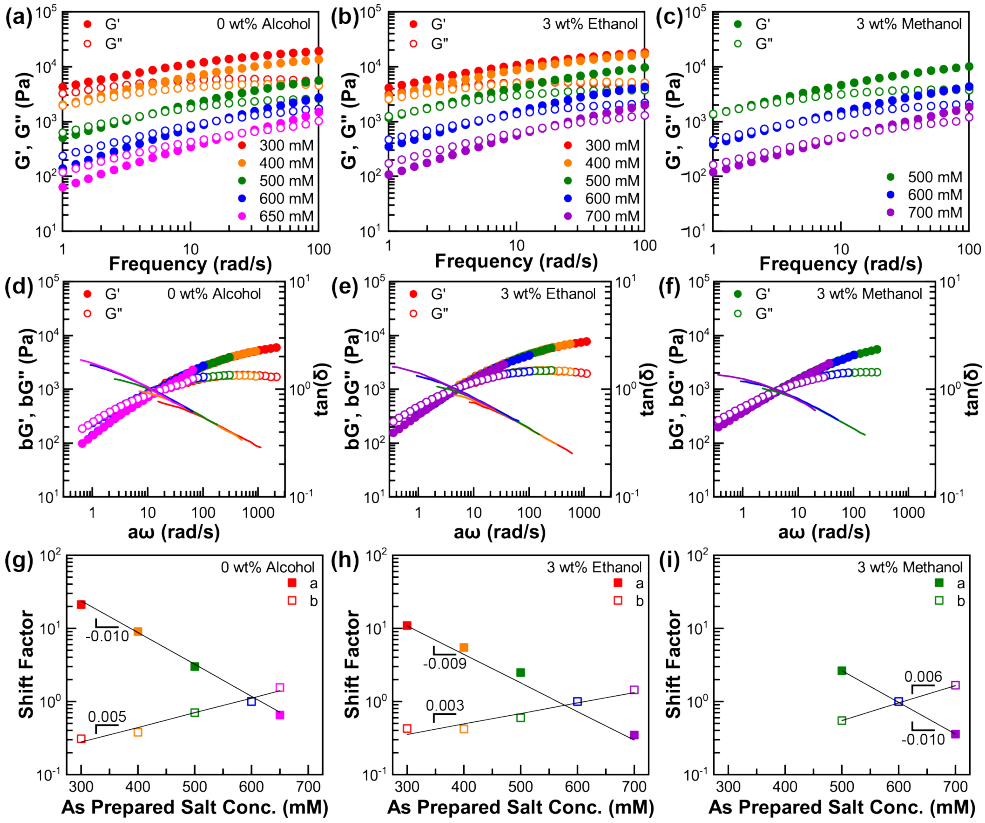

Figure 3. Frequency sweep data for coacervates formed at varying salt concentrations in **(a)** water, **(b)** 3 wt% ethanol, and **(c)** 3 wt% methanol, along with the corresponding **(d-f)** the corresponding time-salt superposition plots and **(g-i)** graphs of the horizontal and vertical shift factors. The data from 600 mM NaCl for each sample was used as the reference for the

superposition. The exponential dependence of the shift factors as a function of the as prepared salt concentration is indicated as the slope of the linear fit on the semi-log plots.

To understand the effect of cosolvents on the rheology of our chitosan-hyaluronic acid coacervates, we also characterized the frequency-dependent linear viscoelasticity as a function of increasing concentrations of both methanol and ethanol across a range of different salt concentrations (Figures 4a,b and S5a-c, S6a-e). We observed a trend of increasing modulus with increasing alcohol concentration, as well as a shift in the crossover point to lower frequencies. Furthermore, we observed slightly higher moduli for samples prepared in ethanol as compared to methanol. These results support the idea of dielectric-induced stiffening of the material and slowing of relaxation dynamics via strengthened electrostatic interactions.

The observation of slightly higher modulus for ethanol-containing samples compared to methanol is interesting in the context of our characterization of the phase behavior of these materials. In particular, at the same total polymer concentration, we observed a lower salt resistance for ethanol-based samples than those containing methanol. At first glance, this salt resistance data might appear to be incongruent with our rheological results, if one makes the assumption that the slope of the tie-lines in the phase diagrams for methanol and ethanol coacervates is the same, and therefore that the composition of the coacervate scales directly with the observed differences in the salt resistance. In the absence of cosolvent effects, the rheological response of a coacervate has been shown to be dominated by the concentration of polymer present in the dense phase.[33] Therefore, one would not expect a coacervate with a lower salt resistance (assuming this correlates to a lower polymer concentration in the coacervate) to have a higher modulus. However, broader consideration of the interactions between polymer,

solvent, and salts has shown that differences in these interactions can lead to differences in the slope of tie-lines, and therefore differences in the composition of the coacervate.[33] Additionally, the presence of alcohols as a cosolvent further raises the possibility of differences in the partitioning of both salt and cosolvent into the coacervate phase, along with the attendant effects on polymer concentration. Further work that fully characterizes the composition of polymer, salt, and cosolvent is necessary to fully understand these observations, but is beyond the scope of the current work. Instead, we looked to identify potentially interesting trends that could be more fully elucidated in a study conducted using model synthetic polymers.

In much the same way that increased salt concentration allows for time-salt superposition by decreasing the inter-chain friction in coacervates while not otherwise altering the self-similarity of the materials, we looked to see if it would be possible to perform a time-alcohol superposition. While the same caveats exist regarding deviations in the tan(δ) curves at the low frequency limit of each dataset, we were very excited to obtain master curves for chitosan/hyaluronic acid coacervates suggesting the possible relevance of cosolvent-related superposition methods (Figures 4c,d and S5d-f, S6f-j). Cole-Cole plots again confirm the quality of our superpositions (Figure S8), though we acknowledge that the limited frequency range of our experiments means that deviations in the time-alcohol superposition at low frequencies could be possible.[64] To the best of our knowledge, this is the first report of time-cosolvent superposition as a concept for understanding the rheology of complex coacervates.

Whereas the horizontal (a) shift factor associated with time-salt superposition showed a trend of decreasing magnitude with increasing salt concentration because of

salt-induced softening of the material, we observed a trend of increasing horizontal shift factor (α) with increasing alcohol concentration because of dielectric-induced stiffening (Figure 4e and S5g-i, S6k-o). Relatedly, while increasing salt concentration is expected to swell the coacervate, thereby decreasing the polymer concentration, stronger electrostatic interactions because of a decreased dielectric constant would be expected to increase the polymer concentration. Thus, while time-salt superposition shows a trend of increasing vertical shift factor (b) with increasing salt, we observed a decrease in the vertical shift factor (β) with increasing alcohol concentration.

The same trends can be observed when considered as a function of dielectric constant (Figures 4f and S5j-l, S6p-t). However, at this time the use of alcohol concentration, rather than dielectric constant appears to allow for a more universal description of the scaling behavior, potentially because of the aforementioned considerations such as solvent partitioning and the disruption of water hydrogen bonding networks. The values of the shift factors for both methanol and ethanol at a given salt concentration appear to collapse onto a single curve when considered with respect to alcohol wt% rather than dielectric constant (Figure 4e,f). The reason for this collapse is not immediately apparent, and would be an intriguing question to explore as part of a future study. In particular, given the two-phase nature of complex coacervates it would be important to understand how various cosolvents partition between the coacervate and supernatant phases, thereby altering the actual dielectric constant of the coacervate phase. We hypothesize that the apparent utility of a mass-based concentration measurement may be a fortuitous result, and not universally applicable. Furthermore, it is unclear how the presence of cosolvents might affect the partitioning of salts, and how this more complex

interplay of factors might affect both the phase behavior and the rheological response. Such questions represent interesting areas for future exploration in the field, both from an experimental and a computational perspective.

Similar to the data from time-salt superposition, it is interesting to note that the magnitude of the slope of both the horizontal and vertical shift factors generally increase with increasing as-prepared salt concentration (Figures S5g-l and S6k-t). In this instance, we hypothesize that the increased salt concentration helps to more dramatically decrease the "friction" associated with electrostatic interactions, facilitating faster chain motions. However, as mentioned previously, further experimental and computational studies into these effects should be performed.

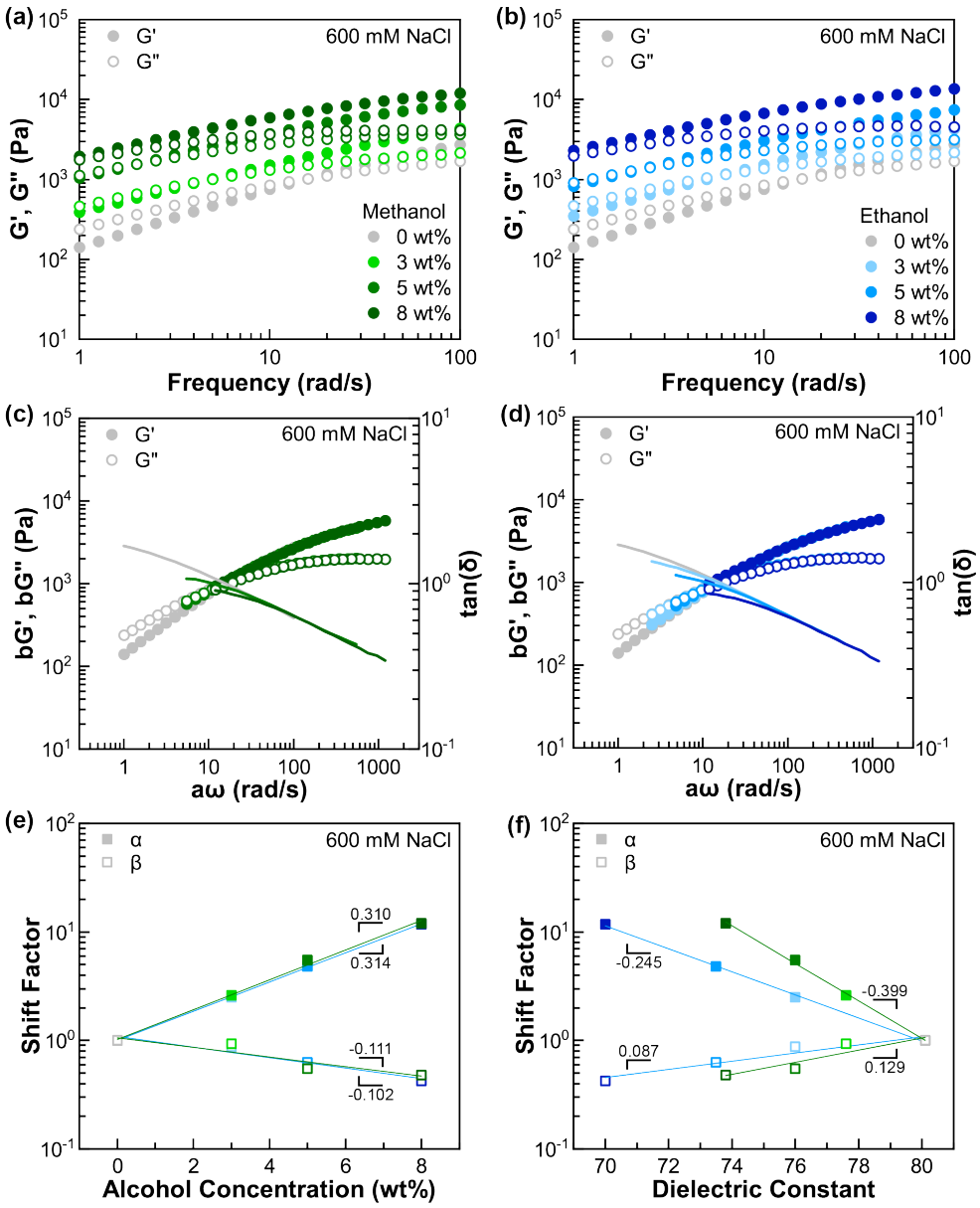

Figure 4. Frequency sweep data for coacervates formed at varying alcohol concentrations and 600 mM NaCl in **(a)** ethanol and **(b)** methanol, and **(c-d)** the corresponding time-alcohol superposition plots and graphs of the horizontal and vertical shift factors as a function of **(e)** alcohol concentration and **(f)** dielectric constant. The data from water-only sample was used as

the reference for the superposition. The exponential dependence of the shift factors is indicated as the slope of the linear fit on the semi-log plots.

Lastly, given the potential to perform both time-salt and time-alcohol superpositions on our data, we explored the possibility of creating a universal master curve via time-salt-alcohol superposition. Again, acknowledging the deviations in tan(δ), but buoyed by the strong superposition observed in Cole-Cole plots (Figure S9), we were very excited to observe not only a superposition of the various salt and alcohol concentrations for our two cosolvent systems (Figure 5b,c), but also a superposition of the data across alcohols (Figure 5a). It will be interesting for future studies to explore the possibility of this more complex superposition using model polymers in a more idealized setting, and to determine whether this seemingly universal behavior is only relevant at low concentrations of relatively similar cosolvents, and how the behavior might change as a function of polymer and solvent chemistry.

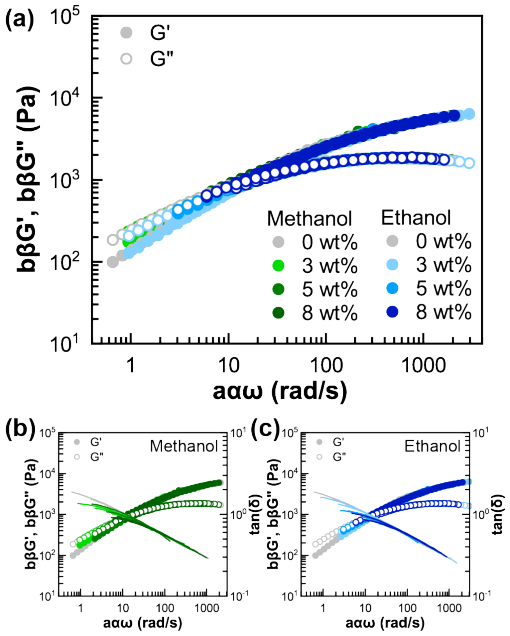

Figure 5. (a) Time-salt-alcohol superposition comparing data across added cosolvent and salt concentrations, along with the individual datasets for **(b)** methanol and **(c)** ethanol.

4. Conclusion

In summary, we describe the time-salt superposition of the linear viscoelastic response of complex coacervates formed from chitosan and hyaluronic acid. Furthermore, we describe the first example of both time-alcohol and time-salt-alcohol superposition as potential strategies for more broadly understanding the effects of Coulombic interactions on coacervate materials. Our systematic analysis highlights the potential for using added cosolvents as an orthogonal approach for modulating the rheology and phase behavior of complex coacervates, and lays the groundwork for extending these efforts to enable the broader design of coacervate materials.

While the addition of alcohol to coacervates of chitosan and hyaluronic acid in this study resulted in trends that could be described in the context of changing dielectric

constant and electrostatic interactions, several recent reports have described the potential for using cosolvent mixtures to improve the solubility of more hydrophobic polyelectrolytes.[58,59] Thus, we suggest that future efforts explore both the effect of polymer and solvent chemistry, using carefully designed model systems, with a goal towards elucidating the underlying physics. We anticipate that solvent effects can be described in terms of three possible contributions: (i) modulating electrostatic effects, (ii) changes in the polymer solubility, and (iii) changes in the structuring of water. Furthermore, while this work focused exclusively on the addition of an organic cosolvent, we propose that the underlying physics needed to understand cosolvent effects can also be used to describe the effect of varying the identity of added salt and/or the specific chemistry of the ionized groups on the various polyelectrolytes.

Associated Content

Supporting Information

Supporting Information describing the physical properties of the solvents used in this study, estimated dielectric constants, frequency sweep data as a function of salt and cosolvent content, along with the corresponding time-salt and/or time-alcohol superposition curves, the corresponding shift factors, and the related Cole-Cole plots.

Author Information

Corresponding Authors

Jessica D. Schiffman – Department of Chemical Engineering, University of Massachusetts Amherst, Amherst, MA 01003, USA; Email: schiffman@ecs.umass.edu

Sarah L. Perry – Department of Chemical Engineering, University of Massachusetts Amherst, Amherst, MA 01003, USA; Email: perrys@engin.umass.edu

Authors

Juanfeng Sun – Department of Chemical Engineering, University of Massachusetts Amherst, Amherst, MA 01003, USA

Author Contributions

The manuscript was written through contributions of all authors. All authors have given approval to the final version of the manuscript.

Notes

The authors declare no competing financial interest.

Acknowledgements

We acknowledge the support of the National Science Foundation (NSF CMMI-1727660). We would also like to thank Drs. Xiangxi (Zoey) Meng, Yalin Liu, Alfred Crosby, and David Hoagland for helpful discussions.

References

(1) Sing, C. E.; Perry, S. L. Recent progress in the science of complex coacervation. *Soft Matter* **2020**, *16* (12), 2885–2914 DOI: 10.1039/D0SM00001A.

(2) Srivastava, S.; Tirrell, M. V. Polyelectrolyte Complexation. In *Advances in Chemical Physics*; Rice, S. A., Dinner, A. R., Eds.; John Wiley & Sons, Inc.: Hoboken, NJ, USA, 2016.

(3) van der Gucht, J.; Spruijt, E.; Lemmers, M.; Cohen Stuart, M. A. Polyelectrolyte complexes: bulk phases and colloidal systems. *J. Colloid Interface Sci.* **2011**, *361* (2), 407–422 DOI: 10.1016/j.jcis.2011.05.080.

(4) Stewart, R. J.; Wang, C. S.; Shao, H. Complex coacervates as a foundation for synthetic underwater adhesives. *Adv. Colloid Interface Sci.* **2011**, *167* (1-2), 85–93 DOI:

10.1016/j.cis.2010.10.009.
(5) Zhang, L.; Lipik, V.; Miserez, A. Complex coacervates of oppositely charged co-polypeptides inspired by the sandcastle worm glue. *J. Mater. Chem. B* **2016**, *4*, 1544–1556 DOI: 10.1039/C5TB02298C.
(6) Hwang, D. S.; Zeng, H.; Srivastava, A.; Krogstad, D. V.; Tirrell, M.; Israelachvili, J. N.; Waite, J. H. Viscosity and interfacial properties in a mussel-inspired adhesive coacervate. *Soft Matter* **2010**, *6* (14), 3232–3236 DOI: 10.1039/c002632h.
(7) Dompé, M.; Cedano-Serrano, F. J.; Vahdati, M.; van Westerveld, L.; Hourdet, D.; Creton, C.; van der Gucht, J.; Kodger, T.; Kamperman, M. Underwater Adhesion of Multiresponsive Complex Coacervates. *Adv. Mater. Interfaces* **2020**, *7* (4), 1901785 DOI: 10.1002/admi.201901785.
(8) McClements, D. J.; Decker, E. A.; Park, Y.; Weiss, J. Structural Design Principles for Delivery of Bioactive Components in Nutraceuticals and Functional Foods. *Crit. Rev. Food Sci. Nutr.* **2009**, *49* (6), 577–606 DOI: 10.1080/10408390902841529.
(9) Schmitt, C.; Turgeon, S. L. Protein/Polysaccharide Complexes and Coacervates in Food Systems. *Adv. Colloid Interface Sci.* **2011**, *167* (1-2), 63–70 DOI: 10.1016/j.cis.2010.10.001.
(10) Kalantar, T. H.; Tucker, C. J.; Zalusky, A. S.; Boomgaard, T. A.; Wilson, B. E.; Ladika, M.; Jordan, S. L.; Li, W. K.; Xhang, X. High throuhgput workflow for coacervate formation and characterization in shampoo systems. *J. Cosmet. Sci.* **2007**, *58* (4), 375–383.
(11) Blocher, W. C.; Perry, S. L. Biomimetic Complex Coacervate-Based Materials for Biomedicine. *WIREs Nanomedicine and Nanobiotechnology* **2017**, *9* (4), e1442 DOI: 10.1021/bm900373c.
(12) Johnson, N. R.; Wang, Y. Coacervate delivery systems for proteins and small molecule drugs. *Expert Opin. Drug Discovery* **2014**, *11* (12), 1829–1832 DOI: 10.1517/17425247.2014.941355.
(13) Mi, X.; Blocher McTigue, W. C.; Joshi, P. U.; Bunker, M. K.; Heldt, C. L.; Perry, S. L. Thermostabilization of viruses via complex coacervation. *Biomater. Sci.* **2020**, *8* (24), 7082–7092 DOI: 10.1039/D0BM01433H.
(14) Kataoka, K.; Harada, A.; Nagasaki, Y. Block copolymer micelles for drug delivery: design, characterization and biological significance. *Adv. Drug Delivery Rev.* **2001**, *47* (1), 113–131 DOI: 10.1016/S0169-409X(00)00124-1.
(15) Meng, X.; Perry, S. L.; Schiffman, J. D. Complex Coacervation: Chemically Stable Fibers Electrospun from Aqueous Polyelectrolyte Solutions. *ACS Macro Lett.* **2017**, *6*, 505–511 DOI: 10.1021/acsmacrolett.7b00173.
(16) Meng, X.; Schiffman, J. D.; Perry, S. L. Electrospinning Cargo-Containing Polyelectrolyte Complex Fibers: Correlating Molecular Interactions to Complex Coacervate Phase Behavior and Fiber Formation. *Macromolecules* **2018**, *51* (21), 8821–8832 DOI: 10.1021/acs.macromol.8b01709.
(17) Meng, X.; Du, Y.; Liu, Y.; Coughlin, E. B.; Perry, S. L.; Schiffman, J. D. Electrospinning Fibers from Oligomeric Complex Coacervates: No Chain Entanglements Needed. *Macromolecules* **2021**, *54*, 5033–5042 DOI: 10.1021/acs.macromol.1c00397.
(18) Sun, J.; Perry, S. L.; Schiffman, J. D. Electrospinning Nanofibers from Chitosan/Hyaluronic Acid Complex Coacervates. *Biomacromolecules* **2019**, *20* (11),

4191–4198 DOI: 10.1021/acs.biomac.9b01072.
(19) Kurtz, I. S.; Sui, S.; Hao, X.; Huang, M.; Perry, S. L.; Schiffman, J. D. Bacteria-Resistant, Transparent, Free-Standing Films Prepared from Complex Coacervates. *ACS Appl. Bio Mater.* **2019**, *2* (9), 3926–3933 DOI: 10.1021/acsabm.9b00502.
(20) Kelly, K. D.; Schlenoff, J. B. Spin-Coated Polyelectrolyte Coacervate Films. *ACS Appl. Mater. Interfaces* **2015**, *7* (25), 13980–13986 DOI: 10.1021/acsami.5b02988.
(21) Basu, S.; Plucinski, A.; Catchmark, J. M. Sustainable barrier materials based on polysaccharide polyelectrolyte complexes. *Green Chem.* **2017**, *19* (17), 4080–4092 DOI: 10.1039/c7gc00991g.
(22) Haile, M.; Sarwar, O.; Henderson, R.; Smith, R.; Grunlan, J. C. Polyelectrolyte Coacervates Deposited as High Gas Barrier Thin Films. *Macromol. Rapid Commun.* **2017**, *38* (1), 1600594 DOI: 10.1002/marc.201600594.
(23) Sadman, K.; Delgado, D. E.; Won, Y.; Wang, Q.; Gray, K. A.; Shull, K. R. Versatile and High-Throughput Polyelectrolyte Complex Membranes via Phase Inversion. *ACS Appl. Mater. Interfaces* **2019**, *11* (17), 16018–16026 DOI: 10.1021/acsami.9b02115.
(24) Priftis, D.; Laugel, N.; Tirrell, M. Thermodynamic Characterization of Polypeptide Complex Coacervation. *Langmuir* **2012**, *28* (45), 15947–15957 DOI: 10.1021/la302729r.
(25) Chang, L.-W.; Lytle, T. K.; Radhakrishna, M.; Madinya, J. J.; Vélez, J.; Sing, C. E.; Perry, S. L. *Sequence and Entropy-Based Control of Complex Coacervates*. *Nat. Commun.* **2017**, *8*, 1273 DOI: 10.1038/s41467-017-01249-1.
(26) Bucur, C. B.; Sui, Z.; Schlenoff, J. B. Ideal Mixing in Polyelectrolyte Complexes and Multilayers: Entropy Driven Assembly. *J. Am. Chem. Soc.* **2006**, *128* (42), 13690–13691 DOI: 10.1021/ja064532c.
(27) Fu, J.; Schlenoff, J. B. Driving Forces for Oppositely Charged Polyion Association in Aqueous Solutions: Enthalpic, Entropic, but Not Electrostatic. *J. Am. Chem. Soc.* **2016**, *138* (3), 980–990 DOI: 10.1021/jacs.5b11878.
(28) Priftis, D.; Tirrell, M. Phase behaviour and complex coacervation of aqueous polypeptide solutions. *Soft Matter* **2012**, *8* (36), 9396–9405 DOI: 10.1039/c2sm25604e.
(29) Perry, S. L.; Li, Y.; Priftis, D.; Leon, L.; Tirrell, M. The effect of salt on the complex coacervation of vinyl polyelectrolytes. *Polymers* **2014**, *6* (6), 1756–1772 DOI: 10.3390/polym6061756.
(30) Priftis, D.; Xia, X.; Margossian, K. O.; Perry, S. L.; Leon, L.; Qin, J.; de Pablo, J. J.; Tirrell, M. Ternary, tunable polyelectrolyte complex fluids driven by complex coacervation. *Macromolecules* **2014**, *47* (9), 3076–3085 DOI: 10.1021/ma500245j.
(31) Chollakup, R.; Beck, J. B.; Dirnberger, K.; Tirrell, M.; Eisenbach, C. D. Polyelectrolyte Molecular Weight and Salt Effects on the Phase Behavior and Coacervation of Aqueous Solutions of Poly(acrylic acid) Sodium Salt and Poly(allylamine) Hydrochloride. *Macromolecules* **2013**, *46* (6), 2376–2390 DOI: 10.1021/ma202172q.
(32) Chollakup, R.; Smitthipong, W.; Eisenbach, C. D.; Tirrell, M. Phase Behavior and Coacervation of Aqueous Poly(acrylic acid)−Poly(allylamine) Solutions. *Macromolecules* **2010**, *43* (5), 2518–2528 DOI: 10.1021/ma902144k.
(33) Liu, Y.; Santa Chalarca, C. F.; Carmean, R. N.; Olson, R. A.; Madinya, J.; Sumerlin, B. S.; Sing, C. E.; Emrick, T.; Perry, S. L. Effect of Polymer Chemistry on the Linear Viscoelasticity of Complex Coacervates. *Macromolecules* **2020**, *53* (18), 7851–7864 DOI: 10.1021/acs.macromol.0c00758.

(34) Spruijt, E.; Westphal, A. H.; Borst, J. W.; Cohen Stuart, M. A.; van der Gucht, J. Binodal Compositions of Polyelectrolyte Complexes. *Macromolecules* **2010**, *43* (15), 6476–6484 DOI: 10.1021/ma101031t.
(35) Spruijt, E.; Cohen Stuart, M. A.; van der Gucht, J. Linear Viscoelasticity of Polyelectrolyte Complex Coacervates. *Macromolecules* **2013**, *46* (4), 1633–1641 DOI: 10.1021/ma301730n.
(36) Priftis, D.; Megley, K.; Laugel, N.; Tirrell, M. Complex Coacervation of Poly (ethylene-imine)/Polypeptide Aqueous Solutions: Thermodynamic and Rheological Characterization. *J. Colloid Interface Sci.* **2013**, *398*, 39–50 DOI: 10.1016/j.jcis.2013.01.055.
(37) Li, L.; Srivastava, S.; Andreev, M.; Marciel, A. B.; de Pablo, J. J.; Tirrell, M. V. Phase Behavior and Salt Partitioning in Polyelectrolyte Complex Coacervates. *Macromolecules* **2018**, *51* (8), 2988–2995 DOI: 10.1021/acs.macromol.8b00238.
(38) Akkaoui, K.; Yang, M.; Digby, Z. A.; Schlenoff, J. B. Ultraviscosity in entangled polyelectrolyte complexes and coacervates. *Macromolecules* **2020**, *53*, 4234–4246 DOI: 10.1021/acs.macromol.0c00133.
(39) Hamad, F. G.; Chen, Q.; Colby, R. H. Linear Viscoelasticity and Swelling of Polyelectrolyte Complex Coacervates. *Macromolecules* **2018**, *51* (15), 5547–5555 DOI: 10.1021/acs.macromol.8b00401.
(40) Momeni, A.; Filiaggi, M. J. Rheology of polyphosphate coacervates. *J. Rheol.* **2016**, *60* (1), 25–34 DOI: 10.1122/1.4935127.
(41) Spruijt, E.; Sprakel, J.; Lemmers, M.; Stuart, M. A. C.; van der Gucht, J. Relaxation Dynamics at Different Time Scales in Electrostatic Complexes: Time-Salt Superposition. *Phys. Rev. Lett.* **2010**, *105* (20), 208301 DOI: 10.1103/PhysRevLett.105.208301.
(42) Tabandeh, S.; Leon, L. Engineering Peptide-Based Polyelectrolyte Complexes with Increased Hydrophobicity. *Molecules* **2019**, *24* (5), 868 DOI: 10.3390/molecules24050868.
(43) Lou, J.; Friedowitz, S.; Qin, J.; Xia, Y. Tunable Coacervation of Well-Defined Homologous Polyanions and Polycations by Local Polarity. *ACS Central Science* **2019**, *5* (3), 549–557 DOI: 10.1021/acscentsci.8b00964.
(44) Huang, J.; Morin, F. J.; Laaser, J. E. Charge-Density-Dominated Phase Behavior and Viscoelasticity of Polyelectrolyte Complex Coacervates. *Macromolecules* **2019**, *52* (13), 4957–4967 DOI: 10.1021/acs.macromol.9b00036.
(45) Fu, J.; Fares, H. M.; Schlenoff, J. B. Ion-Pairing Strength in Polyelectrolyte Complexes. *Macromolecules* **2017**, *50* (3), 1066–1074 DOI: 10.1021/acs.macromol.6b02445.
(46) Perry, S. L.; Leon, L.; Hoffmann, K. Q.; Kade, M. J.; Priftis, D.; Black, K. A.; Wong, D.; Klein, R. A.; Pierce, C. F. I.; Margossian, K. O.; Whitmer, J. K.; Qin, J.; de Pablo, J. J.; Tirrell, M. Chirality-selected phase behaviour in ionic polypeptide complexes. *Nat. Commun.* **2015**, *6*, 6052 DOI: 10.1038/ncomms7052.
(47) Pacalin, N. M.; Leon, L.; Tirrell, M. Directing the phase behavior of polyelectrolyte complexes using chiral patterned peptides. *Eur. Phys. J. Spec. Top.* **2016**, *225* (8-9), 1805–1815 DOI: 10.1140/epjst/e2016-60149-6.
(48) Vieregg, J. R.; Lueckheide, M.; Marciel, A. B.; Leon, L.; Bologna, A. J.; Rivera, J. R.; Tirrell, M. V. Oligonucleotide–Peptide Complexes: Phase Control by Hybridization. *J. Am. Chem. Soc.* **2018**, *140* (5), 1632–1638 DOI: 10.1021/jacs.7b03567.

(49) Li, L.; Rumyantsev, A. M.; Srivastava, S.; Meng, S.; de Pablo, J. J.; Tirrell, M. V. Effect of Solvent Quality on the Phase Behavior of Polyelectrolyte Complexes. *Macromolecules* **2021**, *54*, 105–114 DOI: 10.1021/acs.macromol.0c01000.
(50) Johnston, B. M.; Johnston, C. W.; Letteri, R. A.; Lytle, T. K.; Sing, C. E.; Emrick, T.; Perry, S. L. The effect of comb architecture on complex coacervation. *Org. Biomol. Chem.* **2017**, *15* (36), 7630–7642 DOI: 10.1021/bm201113y.
(51) Tekaat, M.; Bütergerds, D.; Schönhoff, M.; Fery, A.; Cramer, C. Scaling properties of the shear modulus of polyelectrolyte complex coacervates: a time-pH superposition principle. *Phys. Chem. Chem. Phys.* **2015**, *17*, 22552–22556 DOI: 10.1039/C5CP02940F.
(52) Li, L.; Srivastava, S.; Meng, S.; Ting, J. M.; Tirrell, M. V. Effects of Non-Electrostatic Intermolecular Interactions on the Phase Behavior of pH-Sensitive Polyelectrolyte Complexes. *Macromolecules* **2020**, *53*, 7835–7844 DOI: 10.1021/acs.macromol.0c00999.
(53) Wang, Q.; Schlenoff, J. B. The Polyelectrolyte Complex/Coacervate Continuum. *Macromolecules* **2014**, *47* (9), 3108–3116 DOI: 10.1021/ma500500q.
(54) Marciel, A. B.; Srivastava, S.; Tirrell, M. V. Structure and rheology of polyelectrolyte complex coacervates. *Soft Matter* **2018**, *14* (13), 2454–2464 DOI: 10.1039/c7sm02041d.
(55) Liu, Y.; Momani, B.; Winter, H. H.; Perry, S. L. Rheological characterization of liquid-to-solid transitions in bulk polyelectrolyte complexes. *Soft Matter* **2017**, *13* (40), 7332–7340 DOI: 10.1039/C7SM01285C.
(56) Ali, S.; Prabhu, V. Relaxation Behavior by Time-Salt and Time-Temperature Superpositions of Polyelectrolyte Complexes from Coacervate to Precipitate. *Gels* **2018**, *4* (1), 11 DOI: 10.1103/PhysRevE.94.012611.
(57) Syed, V. M. S.; Srivastava, S. Time–ionic strength superposition: A unified description of chain relaxation dynamics in polyelectrolyte complexes. *ACS Macro Lett.* **2020**, *9*, 1067–1073 DOI: 10.1021/acsmacrolett.0c00252.
(58) Danielsen, S. P. O.; Nguyen, T.-Q.; Fredrickson, G. H.; Segalman, R. A. Complexation of a Conjugated Polyelectrolyte and Impact on Optoelectronic Properties. *ACS Macro Lett.* **2019**, *8* (1), 88–94 DOI: 10.1021/acsmacrolett.8b00924.
(59) Meng, S.; Liu, Y.; Yeo, J.; Ting, J. M.; Tirrell, M. V. Effect of mixed solvents on polyelectrolyte complexes with salt. **2020**, *298*, 887–894 DOI: 10.1007/s00396-020-04637-0.
(60) Lee, M.; Perry, S. L.; Hayward, R. C. Complex Coacervation of Polymerized Ionic Liquids in Non-aqueous Solvents. *ACS Polymers Au* **2021**, ASAP DOI: 10.1021/acspolymersau.1c00017.
(61) Liu, Y.; Winter, H. H.; Perry, S. L. Linear Viscoelasticity of Complex Coacervates. *Adv. Colloid Interface Sci.* **2017**, *239* (C), 46–60 DOI: 10.1016/j.cis.2016.08.010.
(62) Yang, M.; Shi, J.; Schlenoff, J. B. Control of Dynamics in Polyelectrolyte Complexes by Temperature and Salt. *Macromolecules* **2019**, *52* (5), 1930–1941 DOI: 10.1021/acs.macromol.8b02577.
(63) Sadman, K.; Wang, Q.; Chen, Y.; Keshavarz, B.; Jiang, Z.; Shull, K. R. Influence of Hydrophobicity on Polyelectrolyte Complexation. *Macromolecules* **2017**, *50* (23), 9417–9426 DOI: 10.1021/acs.macromol.7b02031.
(64) Larson, R. G.; Liu, Y.; Li, H. Linear viscoelasticity and time-temperature-salt and other superpositions in polyelectrolyte coacervates. *J. Rheol.* **2021**, *65* (1), 77–102 DOI:

10.1122/8.0000156.
(65) Miranda, D. G.; Malmonge, S. M.; Campos, D. M.; Attik, N. G.; Grosgogeat, B.; Gritsch, K. A chitosan-hyaluronic acid hydrogel scaffold for periodontal tissue engineering. *J. Biomed. Mater. Res., Part B* **2016**, *104* (8), 1691–1702 DOI: 10.1002/jbm.b.33516.
(66) Tan, H.; Chu, C. R.; Payne, K. A.; Marra, K. G. Injectable in situ forming biodegradable chitosan–hyaluronic acid based hydrogels for cartilage tissue engineering. *Biomaterials* **2009**, *30* (13), 2499–2506 DOI: 10.1016/j.biomaterials.2008.12.080.
(67) Kayitmazer, A. B.; Koksal, A. F.; Iyilik, E. K. Complex coacervation of hyaluronic acid and chitosan: effects of pH, ionic strength, charge density, chain length and the charge ratio. *Soft Matter* **2015**, *11*, 8605–8612 DOI: 10.1039/C5SM01829C.
(68) Lytle, T. K.; Chang, L.-W.; Markiewicz, N.; Perry, S. L.; Sing, C. E. Designing Electrostatic Interactions via Polyelectrolyte Monomer Sequence. *ACS Central Science* **2019**, *5* (4), 709–718 DOI: 10.1021/acscentsci.9b00087.
(69) Han, C. D.; Kim, J. K. On the use of time-temperature superposition in multicomponent/ multiphase polymer systems. *Polymer* **1993**, *34* (12), 2533–2539 DOI: 10.1016/0032-3861(93)90585-X.

Table of Contents